Structures 38 (2022) 719–732

Contents lists available at ScienceDirect

Structures

journal homepage: www.elsevier.com/locate/structures

Bridge seismic hazard resilience assessment with ensemble machine learning

Farahnaz Soleimani [a,*], Donya Hajializadeh [b]

[a] Department of Civil and Environmental Engineering, Georgia Institute of Technology, Atlanta, GA, United States
[b] Department of Civil and Environmental Engineering, University of Surrey, Guildford, Surrey GU2 7XH, United Kingdom

ARTICLE INFO

Keywords:
Bridge seismic performance
Ensemble learning
Seismic hazard analysis
Bridge resilience

ABSTRACT

Recent years have seen a paradigm shift in assessing the performance of assets in response to disruptive hazards, in that resilience is seen as a more inclusive and over-arching decision variable. This shift in decision drivers provides a better picture of asset behavior in response to hazardous events such as earthquakes and hurricanes. Since highway bridges are among the most critical and vulnerable components of transportation networks, evaluating their functionality under extreme events leads to well-informed decision-making. Whilst there is an ever-growing interest in resilience-based hazard assessment in a wide range of infrastructure sectors, there is limited attention on identifying resilience drivers as a function of hazard and asset characteristics. To this end, this paper presents a framework for probabilistic resilience assessment of a cohort of common highway bridges subjected to a wide range of ground acceleration intensities. This study presents the first ensemble learning-based predictive model using bagging and boosting techniques to predict resilience index as a function of seismic events and asset characteristics on bridge resilience. The hypermeters and input structure of the predictive model are optimized to reduce complexity and maximize efficiency. The findings show that the proposed model performs with a 75–95% success rate in predicting resilience as a function of structural characteristics and peak ground acceleration. This model provides useful insights on the impact of various parameters and drivers of resilience in concrete box-girder bridges.

1. Introduction

As principal components of transportation infrastructure, highway bridges play a significant role in facilitating communication and reducing traffic. Bridge damage from a catastrophic event may interfere with its functionality that imposes disruption to the partial or entire transportation network. The consequent malfunctioning directly impacts post-earthquake emergency responses to an extended region that affects the socio-economic recovery process. Past seismic events revealed that bridges can be vulnerable to experience severe seismically-induced damages [27,30,43]. Thereby, evaluating the seismic performance of bridges is essential to optimize the recovery process, repair procedure, retrofit decisions, and sustain emergency management. To this end, this paper presents a generalized probabilistic framework for the resilience assessment of bridges using efficient machine learning (ML) approaches.

According to Transport Resilience Review [11], in the context of extreme events, resilience is defined as “the ability of the transport network to withstand the impact of extreme events, to operate in the face of such condition and to recover promptly from its effects”. The main challenge in resilience-based decision-making is the complexity of the resilience concept and the lack of consensus in its definition and means of quantification. Despite resilience’s interchangeable nature and various perceptions of its concept, specific characteristics such as the ability of a system to absorb, recover and/or adapt to disruptive events are shared among different definitions. For example, Butler et al. [5] define resilience as the degree to which the system minimizes the level of service failure magnitude and duration over its design life when subject to exceptional conditions. In another example, Woods [60] defines four main concepts for resilience as I) a rebound from trauma to reach the equilibrium, II) identical to robustness, III) opposite to brittleness, and IV) network architectures that can sustain system ability to adapt to future disruptive situations.

The review of literature on resilience quantification in the engineering sector indicates that the majority of resilience quantification means have revolved around the post-event rebound capability of the

* Corresponding author.
E-mail address: soleimani@gatech.edu (F. Soleimani).

https://doi.org/10.1016/j.istruc.2022.02.013
Received 13 August 2021; Received in revised form 3 February 2022; Accepted 4 February 2022

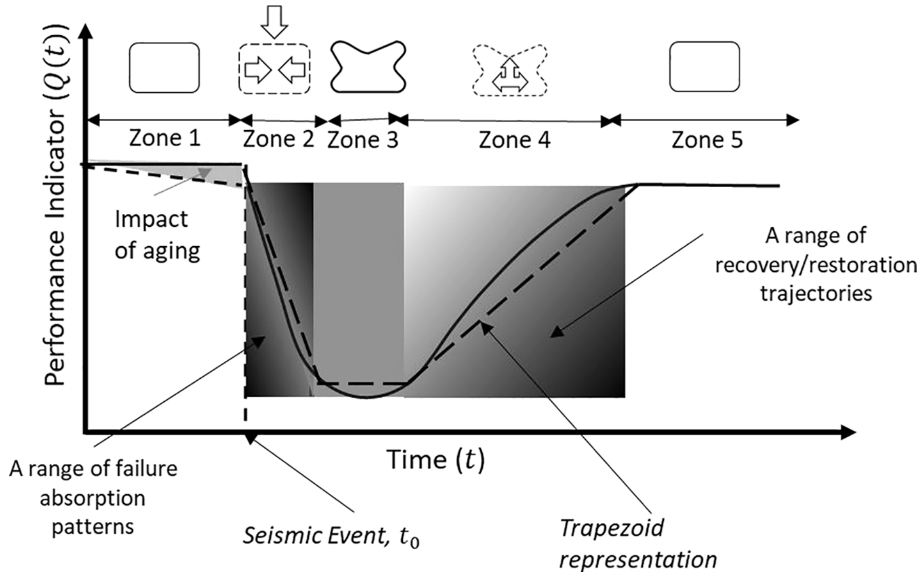

Fig. 1. Schematic illustration of system performance indicator.

asset as a function of time-dependent performance indicator. For example, Henry and Emmanuel Ramirez-Marquez [25] represent the performance changes of a system exposed to a disruptive event as a trapezoid function. In this representation, a system is normally performing at its status-quo equilibrium phase (Zone 1, Fig. 1) and enters the failure absorption phase (Zone 2) at the time when the event happens. Then, the system initiates the recovery phase (Zone 3) and switches to the recovery stage (Zone 4) until reaching the post-recovery equilibrium (Zone 5). Hajializadeh and Imani [20] have used an expanded definition of the trapezoid description to cover more variants of failure absorption patterns and recovery trajectories (Fig. 1).

While there have been limited studies in formulating failure propagation patterns in Zone 2 and considerations for Zone 3, there has been an extensive body of research concentrated on introducing recovery or restoration trajectories, Zone 4. In this regard, as in the overview provided by Gidaris et al. [19], the restoration functions of a bridge subjected to earthquakes can either be derived using probabilistic analytical models or based on experts' judgments. Among the theoretical models, Bocchini et al. [4] proposed a six-parameter sinusoidal function that could capture multiple forms of restoration trajectory such as linear [3,9] and exponential [28]. Furthermore, several researchers such as Decò et al. [12] and Biodini et al. [2] used this function to develop probabilistic resilience assessment considering the uncertainties associated with peak ground acceleration (PGA) intensities and retrofitting process.

In the representation of an asset/structure/infrastructure/system performance as a function of a performance indicator, $Q(t)$, resilience is often measured as a rate of recovery. This definition considers the performance of the asset in Zone 4 only. Another common metric is the area of remaining performance indicator (positive connotation)/area of lost performance indicator (negative connotation). This metric is often formulated and expressed as equation (1):

$$R = \frac{1}{t_h - t_0}\int_{t_0}^{t_h} Q(t)dt \tag{1}$$

in which, R represents the resilience index, t_0 and t_h indicate the start and end of the time horizon considered for the analysis. This technique has been widely used in resilience-based single/multi-hazard assessment frameworks [26,19]. Additional but rarely used metrics include Resilience Density Function, Bandwidth and Resilience Moment, and Cumulative Resilience [46].

Whilst resilience, as defined in the engineering context, has been considered a core decision variable of many of the recent hazard-assessment frameworks, its main drivers and its dependencies on asset characteristics are yet to be investigated. The classical approach to estimate resilience can be improved in several aspects such as improving reliability and prediction power. To this end, the current study includes important sources of uncertainties in the resilience model. The lack of flexibility of the classical approach to incorporate sources of uncertainties into the resilience model can influence the reliability of the estimations. Furthermore, investigating the influence of the variations of uncertain features on the resilience requires a substantial computational cost to re-do bridge seismic analysis with the new set of feature combinations. Thereby, including uncertain configurational features [50] in the quantification of structural resilience is crucial to have a more realistic estimation.

ML approaches provide ample opportunities to enhance the resilience assessment of structures due to their capability to handle complex problems with a large dataset. Taking advantage of the ever-growing computational power offered by ML algorithms, this study presents a novel ensemble learning (EL) – based resilience prediction model. This model predicts resilience index as a function of seismic hazard and bridge structural characteristics. Also, neglecting significant sources of uncertainties could lead to over- or under-estimation of resilience. Therefore, as part of the proposed model in this study, an embedded feature identification technique [53] is used to provide useful insights into the level of influence of the structural features on the bridge resilience and the main structural-based resilience drivers for the first time.

Moreover, the classical resilience models have fixed functional forms and prior assumptions on the distribution of parameters. Consequently, they may not be able to accurately capture complexity in the data due to its high-dimensional nonlinear nature. Hence, a more generalized approach such as EL methods can be especially helpful to model complicated relationships between the input and output data without engineered prior knowledge.

In the ML community, EL methods have been introduced [13] as unbiased algorithms that can capture the complex relationship between the input and response variables. These methods owe their popularity over other ML approaches to reducing model variance with low bias. Furthermore, researchers have successfully applied EL methods to solve a diverse set of research problems [61,22,32,51]. The use of EL algorithms, in this study, is mainly motivated by their unique approach in combining multiple individual learners to achieve an enhanced averaged prediction quality relative to single regression models. Besides, this

Table 1
Description of the damage states [49].

Descriptions	DS1*	DS2*	DS3*	DS4*
Qualitative description of damage	Aesthetic damage	Repairable minor functional damage	Repairable major functional damage	Component replacement
Shake Cast Inspection Priority levels	Low	Medium	Medium-High	High
Likely Immediate Post- Event Traffic State	Open to normal public traffic – No Restrictions	Open to Limited public traffic – speed/ weight/lane restrictions	Emergency vehicles only – speed/ weight/lane restrictions	Closed (until braced) – potential of collapse
Traffic Operation Closure/ detour needed	Very unlikely	Unlikely	Likely	Very likely
Traffic restrictions needed	Unlikely	Unlikely	Very likely	Very likely
Emergency Repair Shoring/ bracing needed	Very unlikely	Unlikely	Likely	Very likely
Roadway leveling needed	Unlikely	Likely	Very likely	Very likely

* DS1, DS2, DS3, and DS4 represent slight, moderate, extreme, and complete damage states.

characteristic aids in reducing the overall prediction error. This approach is particularly beneficial to improve predictions by specifically overcoming challenges such as weak predictors, small sample size, and overfitting training data [21,13]. This study aims to pave the path towards the application of ML algorithms in the seismic resilience assessment of bridges. In summary, the key novelties of the presented investigation lie in two folds: 1. The application of ensemble machine learning in building a bridge resilience assessment framework and 2. Appraisal and quantification of structure-based resilience drivers.

The following section provides a detailed overview of the probabilistic resilience assessment framework utilized in this study. Section 3 presents an overview of the Ensemble Machine Learning approach. Sections 4 and 5 provide details of the EL-based resilience predictive model and its application to a cohort of highway bridges, followed by reflection on results and concluding remarks in Section 5.

2. Seismic resilience assessment framework for bridges

In this study, the resilience index is quantified as the area of remaining functionality (also referred to as a performance indicator), as shown in Fig. 1. To describe the behavior of a bridge in response to a seismic event, the structural capacity is utilized as a performance indicator of the structure also referred as $Q(t)$. Following a seismic event, the structural capacity of the bridge is reduced to the corresponding remaining capacity, Zone 2. The failure absorption pattern in Zone 2 is a function of hazard and structural specifications (i.e., for severe seismic events and brittle behavior, the failure propagation is a sudden drop in performance indicator, whereas for a ductile structure, a more graceful failure absorption is expected). The failure absorption of a structure following a hazardous event (e.g., seismic event) is often simplified as a sudden drop in performance indicators. For seismic hazards, the magnitude of the drop is defined as a function of the damage state [40], that are defined according to the extent of the damage varying from slight to complete (Table 1). The typical four states include slight, moderate, extensive, and complete [16], with their corresponding definitions as provided in Table 1.

To account for a wide range of seismic event intensities, damage levels, and different structural characteristics in failure propagation functions, fragility curves are driven from probabilistic seismic demand models (PSDMs). PSDMs of bridge components (e.g., column, abutment) express engineering demand parameters (EDP) (e.g., column curvature ductility) as a function of the PGA intensity (IM). The common PSDMs is a single variable linear regression model, with regression coefficients a and b, which estimates the median value of EDPs at each IM value (Equation (2)) with the variability expressed in the form of a dispersion value (β_{DM}) as shown in Equation (3) with DM representing the demands data points.

$$\ln(\mu_{DM}) = \ln(a) + b\ln(IM) \tag{2}$$

$$\beta_{DM} = \sqrt{\frac{\sum_{i=1}^{n}[\ln(DM_i) - (\ln(a) + b\ln(IM_i))]^2}{n-2}} \tag{3}$$

This was first introduced by Shome et al. [47] and has been widely applied for the performance analysis of various types of bridges [18,41,62,42,54] over the years. Modified versions of the seismic demand models have been proposed by researchers for the application to bridges with specific characteristics [49,55,52,65].

The seismic demand model is often used to derive parameters required for analytical fragility curves expressed as Equation (4) that shows the probability calculation for the p^{th} bridge component.

$$PF_{p|IM} = P[S_D \geqslant S_C|IM] = \Phi\left(\frac{\ln\left(\mu_{DM}/S_C\right)}{\sqrt{\beta_{DM}^2 + \beta_C^2}}\right) \tag{4}$$

in which $\Phi()$ stands for normal cumulative function, S_C and β_c represent the mean and dispersion of capacity values. In order to estimate the bridge system fragilities, the component fragilities can be combined using a joint probabilistic approach and Monte Carlo simulations as proposed by Nielson and DesRoches [39]. Another technique is to use the upper conservative and lower unconservative bounds (Equation (4)) that provides an approximate probability interval. In this study, the former approach is used.

$$\max_p PF_{p|IM} \leq PF_{system|IM} \leq 1 - \prod_p [1 - PF_{p|IM}] \tag{5}$$

This calculation is built on the assumption that the EDPs are lognormally distributed [35] which may not be an applicable assumption for all types of bridges and EDPs as recently shown by several studies such as [17]. Thereby, establishing a more generalized ML-based framework that does not require such a prior assumption on the distribution of variables is desirable. To this end, EL methods satisfy this criterion by covering a wide range of distributions for the input variables.

Similar to damage absorption patterns, recovery trajectories are often defined as a function of pre-defined four damage levels/states. This study considers the commonly used [63,59,14,29] recovery function recommended by HAZUS-MH [24]. The recovery trajectory is defined as a normal cumulative distribution function, with mean recovery time ($m_{t,d}$) and standard deviations ($\sigma_{t,d}$). The recommended values for $m_{t,d}$ are 0.6, 2.5, 75, 230 days for the slight/minor, moderate, extensive, and complete damage states, respectively. For the standard deviations ($\sigma_{t,d}$) values of 0.6, 2.7, 42, 110 days are recommended for four damage states. Considering the abrupt drop in performance indicator as the failure propagation function and utilizing the defined

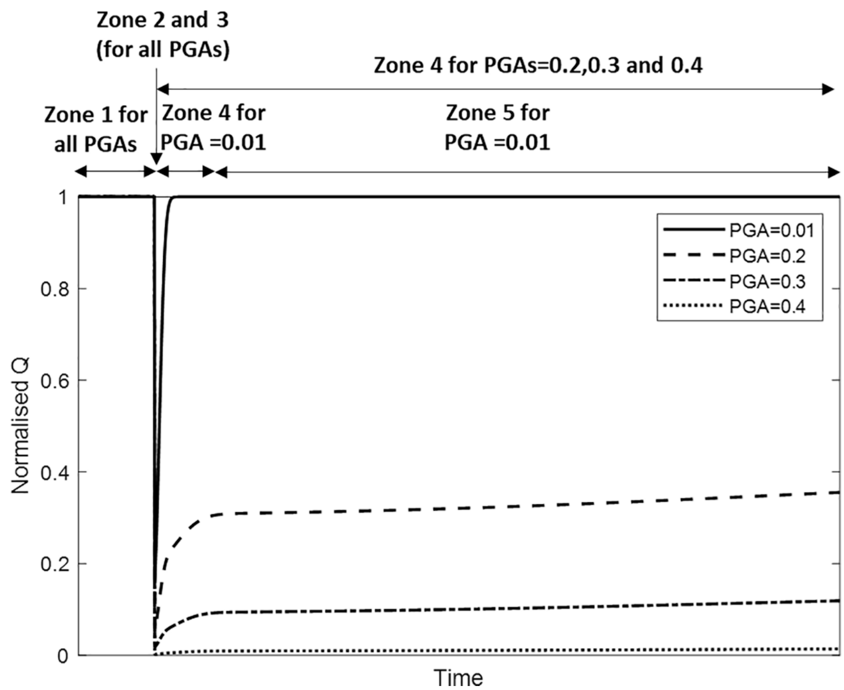

Fig. 2. An example of normalized performance indicator considered in this study.

normal distribution to express recovery trajectory, the normalized performance indicator function in this study can be formulated as shown in Equation (6):

$$\overline{Q}(t) = \sum_{d=1}^{nDs}\left(1 - PF_{p|IM}\right) \times \Phi\left(\frac{t - m_{t,d}}{\sigma_{t,d}}\right) \tag{6}$$

Fig. 2 demonstrates a sample of the considered normalized performance indicator for a range of PGAs. As can be seen from this figure, all performance indicators start with the ideal condition of 100% functionality (Zone 1). As can be expected the duration of recovery is highly dependent on the intensity of the seismic event, therefore the extend of Zone 4 varies with the PGA intensity.

In this representation, the behavior of the asset is formulated from the end of the failure absorption zone, Zone 2, and the recovery initiation time is assumed negligible. It is also assumed that both the failure propagation and recovery trajectory functions share the same conditional probability of occurrence. This can be argued as a reasonable assumption since the recovery trajectory is a function of bridge characteristics and hazard intensity, as is the case with failure propagation.

3. Ensemble machine learning approach

3.1. Overview of the algorithms

A decision tree [6] algorithm that divides data into branch-like segments can be used to solve both classification and regression problems. This non-parametric methodology can efficiently deal with large datasets, complicated data structures, and missing values. Decision trees

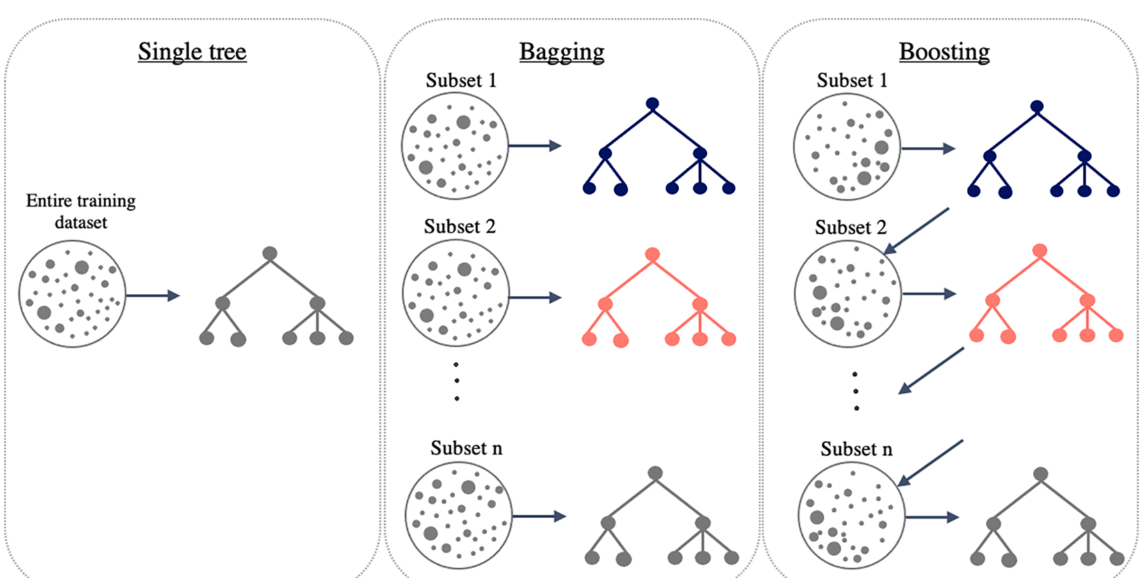

Fig. 3. Schematic diagram of the ensemble learning methods.

Structures 38 (2022) 719–732

provide easy-to-interpret visualizations by constructing an inverted tree with a root node on the top, which represents all the rows in the data set. The root node is divided into child/interior nodes. Nodes that do not have any child are called terminal/leaf nodes. This approach evaluates the GINI index [31] to determine the optimal split of data.

Although individual decision/regression trees generate an intuitive understanding of how the input variables are related to the outputs, they are very sensitive to minor changes in the training data set [13]. The ensemble method provides an efficient tool to overcome this challenge and prevent the overfitting issue [64]. This non-parametric ML technique can be applied to solve a wide range of problems [36] since it does not presume any underlying distribution of the input and output variables. In the EL approach, multiple decision/regression trees are generated and trained in a parallel or sequential manner as base learners [66]. This aggregating strategy can enhance the efficiency of individual learners to improve the accuracy and generalization ability of a predictive model [61].

Two different main techniques known as bagging and boosting can be applied to create base learners. Both methods can produce more flexible and stronger predictive models compared to the single regression trees, however, they differ in functionality. The former primarily reduces the model variance by producing several learners in parallel, whereas the latter reduces the bias by creating sequential learners (Fig. 3). A brief overview of the EL techniques, used in this study, is provided in the following. However, for more detailed explanations, interested readers are encouraged to review provided references in this section and the works by Bühlmann [8], Hastie et al., [23], Skurichina and Duin [48], Sutton [57], and Syam and Kaul [58].

3.1.1. Bagging

Bagging, introduced by Breiman [7], implements bootstraps aggregation to randomly split the entire training data into similar-sized samples with replacements to train multiple independent learners [1,56]. Then, the outputs of all learners are concatenated to compute the final averaged prediction. The generalization error of this method directly depends on the characteristics of the base learners.

3.1.2. Random forest

Random Forest is a bagging supervised technique in which multiple regression trees are constructed in parallel with no interaction between them [33]. The output is the mean prediction of individual regression trees. In order to minimize the correlation between the individual learners in Bagging method, random forest algorithm performs an iterative procedure to randomly select candidate features [23]. To ensure that the constructed individual models consider the potentially predictive candidates rather than heavily relying on any individual feature, random forest uses a random subset of input features to construct trees at each iteration [15]. The optimum subset of features is obtained through cross-validation.

3.1.3. Boosting

While bagging aggregates independent learners, boosting follows a sequential process to create new models based on the preceding learners by correcting their errors iteratively [44,34]. More particularly, this algorithm trains the new learners to fit the residual of previous fits. This leads to a decrease in the bias in addition to reducing the variance. In general, the performance of the final model depends on the number of boosting learners and the total steps, that their optimum values are found by cross-validation.

The subset creation in boosting method depends on the performance of the previous models. More specifically, in the initial round of the subset selection, boosting assigns equal weights to all samples to give all data points an equal chance to be selected. For each subsequent iteration, boosting updates the weights of the samples, so that, samples with wrong or low prediction rates can have a higher probability of being selected for training the new model. In this way, the next hypothesis is more likely to predict those inputs correctly. Ensemble learning eventually combines the whole set to convert all these learners into a better-performing model.

Table 2
Key advantages and disadvantages of EL techniques.

Strategy	Bagging	Random Forest	Boosting
Advantages	• uses Bootstrap sampling method; • the combination of overlapping observations in training helps to overcome high variance; • prevents overfitting in the model;	• produces high accuracy mainly due to its 'wisdom of the crowds' approach; • scales well computationally when new features or samples are added to the dataset; • runs efficiently on large databases; can handle thousands of input variables without variable deletion; • gives estimates of level of importance of variables in regression analysis; • generates an internal unbiased estimate of the generalization error as the forest building progresses; • has an effective method for estimating missing data and maintains accuracy when a large proportion of the data are missing.	• takes care of the weightage of the higher accuracy sample and lower accuracy sample and then gives the combined results; • net error is evaluated in each learning steps. It works good with interactions; • helps when we are dealing with bias or underfitting in the data set;
Disadvantages	• not helpful in case of bias or underfitting in the data; • ignores the value with the highest and the lowest result which may have a wide difference and provides an average result;	• can overfit some datasets with noisy regression tasks; • for data including categorical variables, this technique is biased in favor of those attributes with more levels;	• requires a meticulous tuning of hyperparameters; • often ignores overfitting or variance issues in the data set; • increases time and computation costs;

3.1.4. Application of ensemble learning techniques

Individual regression trees are sensitive to the variability in data that can easily lead to overfitting training data with a tendency to find local optima and are also computationally expensive. EL techniques mitigate these issues by combining the predictions from many decision trees.

Although EL techniques produce higher predictive accuracy, they have their own advantages and weaknesses. In general, EL techniques provide an efficient solution for most problems with nonlinear trends, but they may not be a suitable approach for problems that deal with time series analysis with identification of increasing/decreasing trends. Moreover, implementing EL techniques requires more computational costs to create and train multiple models than a single model. Therefore,

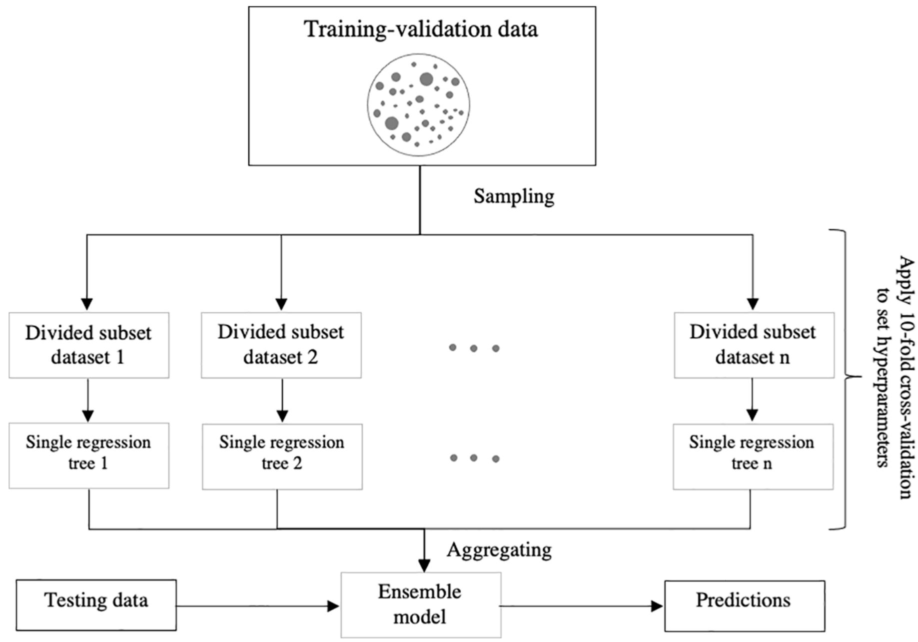

Fig. 4. Supervised ensemble learning procedure.

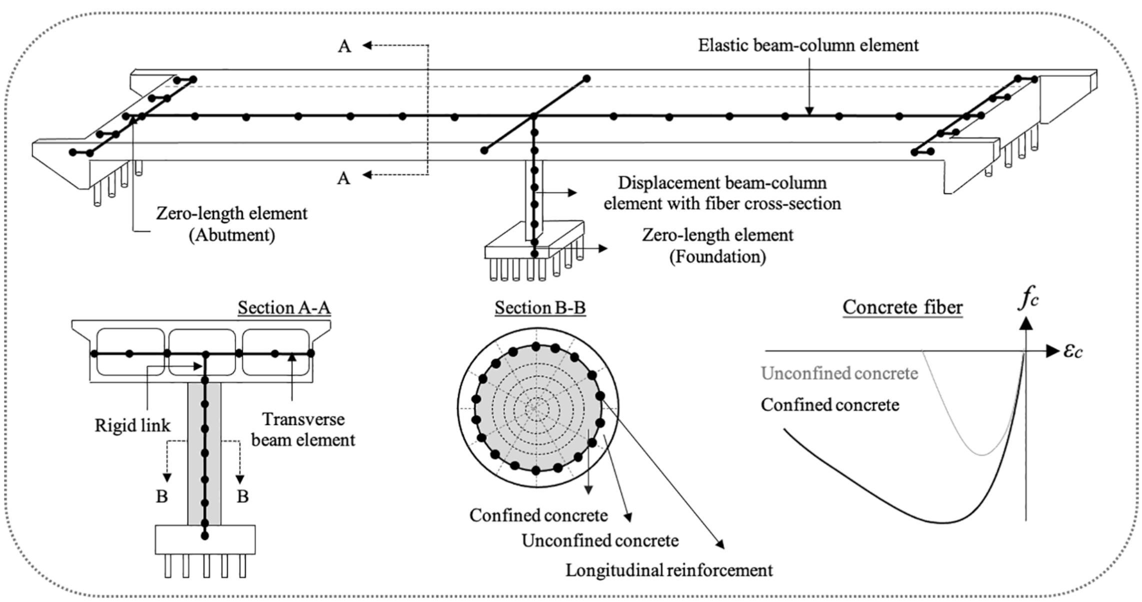

Fig. 5. General layout illustration of the bridge model.

the trade-off between the complexity and the improvement in the prediction accuracy should be optimized based on available resources for a specific problem to solve.

Depending on the problem characteristics, the most suitable EL-based strategy can be selected. For example, a problem with high variance in data would most benefit from following bagging approaches, while boosting would be a great approach to solve a problem involving biased models. Table 2 highlights the key advantages and disadvantages of the different strategies. This study examines the implementation of the three EL-based strategies to test their efficiencies for estimating the seismic resilience of bridges. The comparative analysis of the results is then used to recommend the best-performed model for future applications.

3.2. Implementation of ensemble learning methodology

The initial step in developing predictive models using ML algorithms is to split data into two subsets to train the model and test its performance accordingly. This study randomly allocates 80% and 20% of data to training and testing, respectively.

In the training process, the grid search method is used to combine with 10-fold cross-validation to tune the hyper-parameters such as the depth of the tree, the number of decision trees, and the size of each bag. The *k*-fold cross-validation technique prevents bias in sampling and is commonly used to randomly split *k* equal-sized samples. *k*-1 samples are used to train the model, while the remaining sample (also known as the validation set) is used for model validation to identify the optimum hyperparameters. The hyperparameters that minimize the cross-validation loss are selected. For example, in bagging method, 200 was

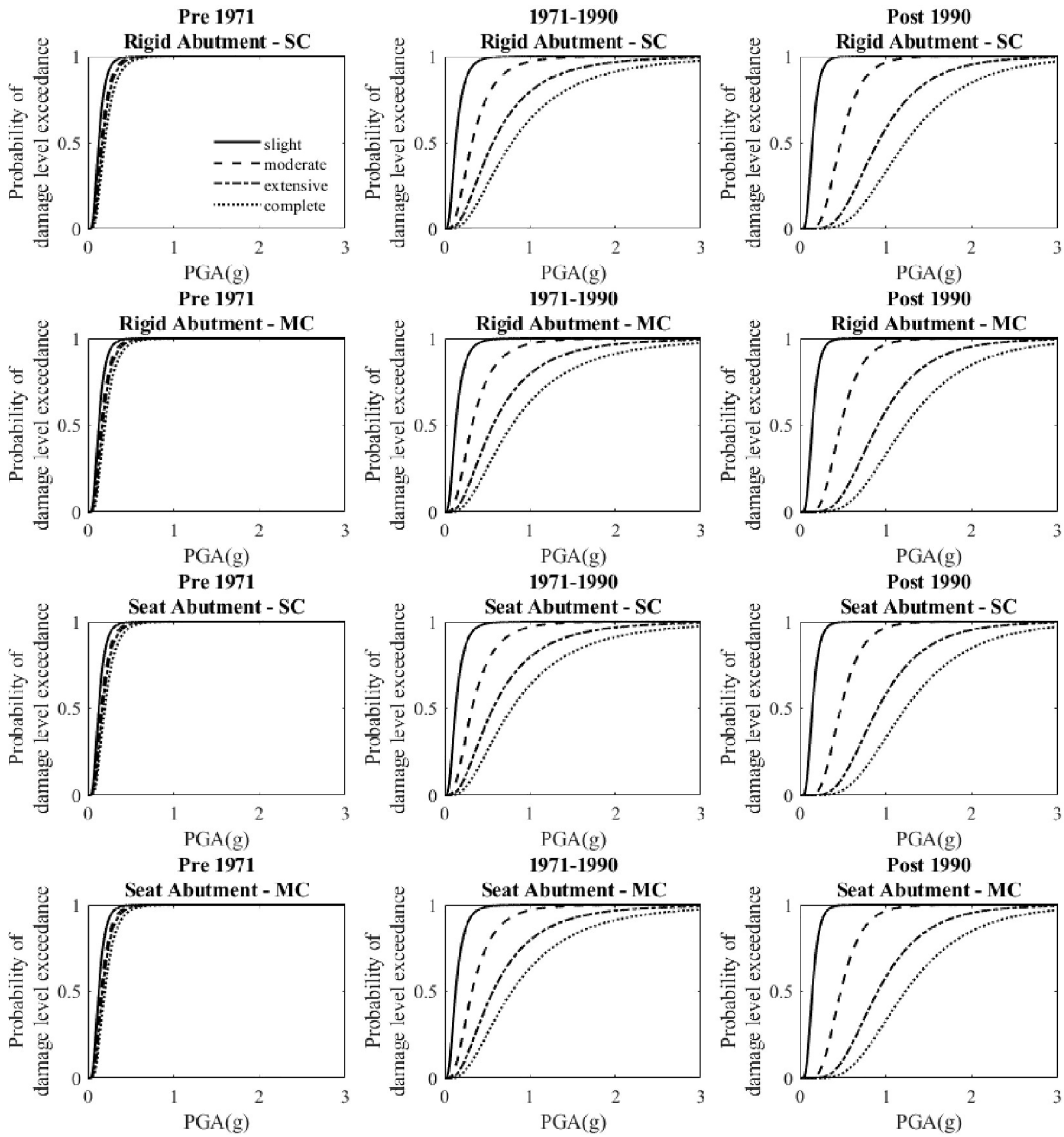

Fig. 6. Fragility curves of the investigated bridges.

found as the best number of learning cycles that results in the minimum mean squared error. The performance of the final models using the testing set is evaluated in terms of quantitative metrics such as prediction accuracy. The general procedure is illustrated in Fig. 4.

4. Illustrative case study

This study considers two-span continuous concrete box-girder highway bridges as a case study, with the configuration demonstrated in Fig. 5, that is representative of a very common bridge class constructed in California. The considered bridges are modeled in three dimensions in OpenSEES. The seismic behavior of bridges is analyzed based on three significant design periods, including pre-1971, 1971–1990, and post-1990 eras and two different bridge portfolios with rigid diaphragm and seat abutments. These eras are defined according to the evolved seismic provisions in designing bridges in response to the deficiencies observed during the historic 1971 San Fernando and the 1989 Loma Prieta earthquakes [45]. The San Fernando earthquake unveiled the necessity of modifying bridge design codes to lower the observed vulnerabilities such as the shear failure of the bridge columns, typically in the plastic hinge region, and the pull-out of the longitudinal reinforcements. Hence, the reinforcement ratio and stirrup detailing have been changed in the later eras to improve the ductility of the columns and encourage columns to experience a ductile failure mode in extreme situations.

This study follows a probabilistic seismic demand analysis by randomly choosing the bridge attributes from their probability distribution (Tables A.1 and A.2 in Appendix A) captured from the NBI [38] and review of bridge drawings. Interested readers are encouraged to find out more details about the analytical modeling procedure and bridge characteristics in other studies on the box-girder concrete bridges [42,49]. In addition to the treatment of uncertainty in the structural

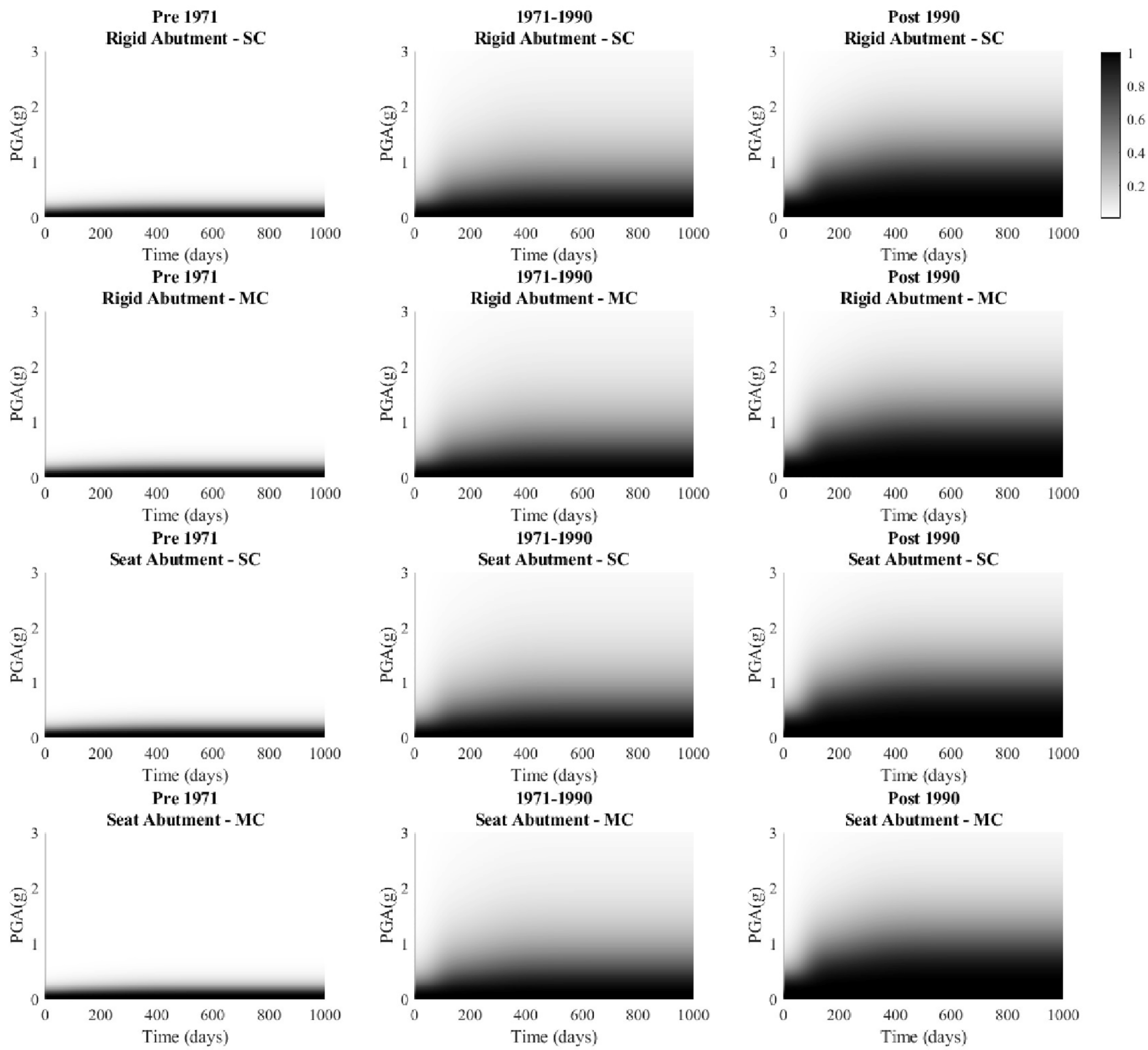

Fig. 7. Normalized performance indicator.

parameters, this study considers the uncertainty associated with the excitations by applying Baker's suite of ground motions, with scaling factors 1 and 2, that covers a broad range of spectral shapes and properties pertinent to California region. This suite corresponds to shallow crustal earthquakes that were assembled for the PEER Transportation Research Program [10]. This study considers the key engineering demand parameters, including the curvature ductility of the columns, deck displacement, foundation rotation and displacement, and abutment displacements (passive, active, and transverse). The limit states or the component capacities [42] that are used in developing the fragility curves are listed in Appendix A (Table A.3).

This study considers the vulnerability of multiple bridge components. Using the finite element models of bridges, the corresponding peak demand measures, such as the column curvature ductility, bearing and abutment deformations, are recorded. Then, PSDMs are developed, and the fragility analysis procedure is employed to generate analytical fragility curves for the bridge components and system. The results are displayed in Fig. 6 for the considered bridge types. Depending on the design eras, box-girder bridges consist of various numbers of column bents. For the pre-1971 era, bridges have either one or two-column bents, while for the later eras including 1971–1990 and post 1990, the number of column bents ranges from one to four and one to five, respectively. Previous studies [37] indicated that the seismic performance of single-column bent (SC) bridges noticeably differs from the multicolumn bents (MC) bridges, and consequently, MC bridges can be classified into a single class based on their similar performance. The median fragilities significantly change from pre-1971 to the other two eras, particularly for the complete damage level. This change is more noticeable for the MC bridges implying the higher impact that the improvements in the seismic design of the columns had on multi-columns which reduces the vulnerability.

5. Application to bridge resilience assessment

5.1. Quantification of bridge resilience and data processing

This section presents the application of the described framework to a realistic case study. Fig. 7 demonstrates the performance indicator, as defined in this study, for a range of bridge types and design codes. This figure shows the performance indicator of the bridge from the moment of seismic event occurrence, hence the sudden drop in performance at time zero. With the initiation of the recovery, the performance indicator starts to grow. Considering a time horizon of 1000 days, the performance indicator in high PGA intensities does not reach the original pre-failure magnitude. As can be expected, the performance indicator of a bridge is reduced with PGA intensity. Fig. 7 shows that the performance

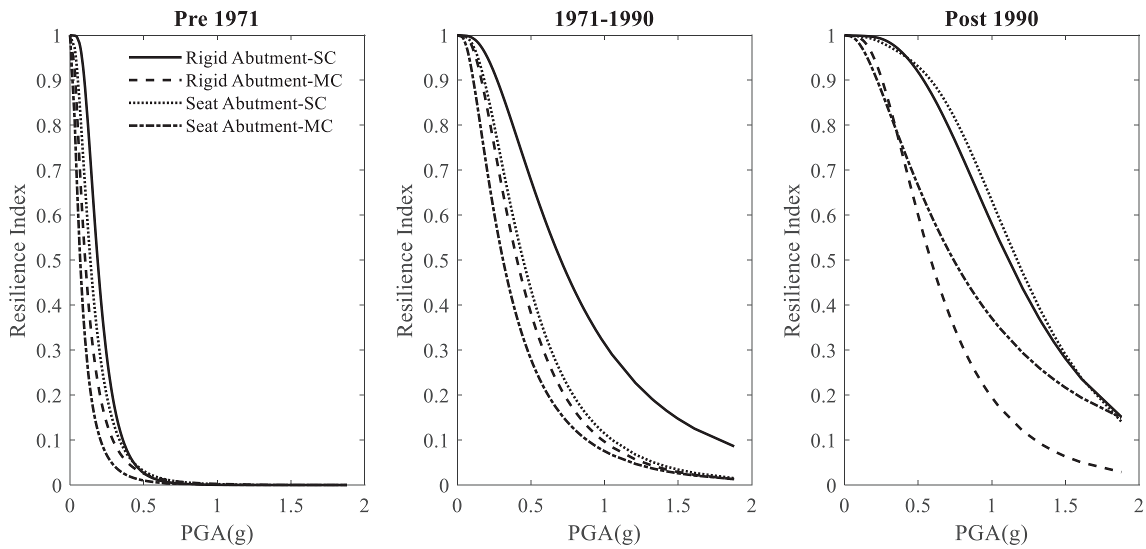

Fig. 8. Resilience Index for selected cohort of bridges.

of bridges designed according to seismic provisions in post 1990 standards is much higher than the same structural forms in pre 1990 eras. This figure also shows that in general rigid/integral abutments outperform seat abutments.

Using the framework presented in Section 2, resilience is calculated for each cohort of fragility curves as shown in Fig. 8. As expected, the considered resilience metric decreases with an increase in the level of earthquake intensity PGA (Fig. 8). This degradation trend is more drastic in the case of bridges designed based on pre-1971 codes. The results show that, by improving the seismic design codes, the resilience of bridges enhances in all scenarios. For example, for the bridge type: pre-1971 with seat abutment with MC, resilience drops to values close to zero at high PGA values, greater than 0.8 g. However, this happens at a later stage (~2.0 g) for the same bridge type that is designed in 1971–1990, while for those that are constructed based on the post-1990 codes, the minimum captured resilience is around 0.2. This is aligned with observations in corresponding fragility curves, in which the probability of damage exceedance in post-1990 bridge designs is much lower than the pre-1971 and 1971–1990.

Fig. 8 also shows that among different structure forms, bridges with SC and rigid/seat abutment demonstrate higher resilience in comparison to MC rigid/seat Abutment. This could be attributed to a variety of factors, such as the differences between the bridge geometries and the fixity conditions. Pinned end conditions are typically used for multi-columns, while the rotational movement is restrained for the single columns. For pre-1971 and 1971–1990 bridge designs, it can be seen that seat abutment offers a lower resilience in comparison to the rigid abutment. The comparison between multi-column bridge cohorts reveals that although seat abutment demonstrates a lower resilience index in seismic intensities less than 0.5 g, it outperforms seat abutment structural form in higher intensities for post-1990 designs. This could be related to the applied retrofitting procedures. For the 1971–1990 era, the primary focus was to improve the performance of the non-ductile columns by steel or fiber jackets. However, the-post 1990 retrofitting program covered a wider range of issues such as increasing the height cap and number of piles for the footings and using longer retainers and seat extenders to prevent the abutment unseating.

To investigate the impact of the fragility curves on the formulated resilience index, Fig. 9 shows resilience index profile vs probability of occurrence for different damage states, different bridge forms, and different seismic provisions. This figure shows that the defined resilience index is predominantly influenced by the fragility curves for the complete damage state. This can be explained by a relatively higher probability of occurrence in this damage state; however, the weight of the influence is reduced considering a lengthier profile of the recovery trajectory for this damage state.

5.2. EL-based resilience models

Each model described in Section 3 is trained with the training dataset for each considered bridge type. For the input variables, a list of sixteen parameters, listed in Table 3, is selected to cover features related to the material, geometric, and structural properties, and PGA, to predict bridge resilience as the outcome. Then, the seismic resilience is estimated for the testing dataset using the trained EL-based models. The predicted resilience values are compared with the analytically derived values obtained following the approach explained in Section 2.

Researchers investigated various IMs in predicting the seismic demand of bridge components considering the metrics including efficiency, practicality, sufficiency, and proficiency. According to these analyses, several studies [41,42] that focused on common bridge portfolios in the risk assessment software package (HAZUS-MH, 201) recommended PGA as the optimal IMs for probabilistic seismic demand analysis of a wide range of bridges. Therefore, for developing the ML-based resilience models, this study adopts PGA to study typical concrete box-girder highway bridges.

This section presents a statistical analysis of the EL-based models to predict resilience. The performance of the three EL algorithms is evaluated in predicting the seismic resilience of the considered cohort of bridges. To assess the prediction performance of the EL-based models, statistical indicators including prediction accuracy (Equation (7)), mean squared prediction error (MSPE) (Equation (8)), and mean absolute prediction error (MAPE) (Equation (9)) are compared. While both MSPE and MAPE provide the averaged magnitude of the error, large errors have higher weights in the MSPE computation than that of MAPE since the first one uses a quadratic score while the latter uses a linear score. Hence, all individual predictions contribute equally to measuring MAPE.

$$\text{Prediction Accuracy} = 1 - \frac{\sqrt{\sum_{i=1}^{n}(\widehat{y}_i - y_i)^2}}{\sqrt{\sum_{i=1}^{n}(y_i)^2}} \tag{7}$$

$$MSPE = \frac{1}{n}\sum_{i=1}^{n}(y_i - \widehat{y}_i)^2 \tag{8}$$

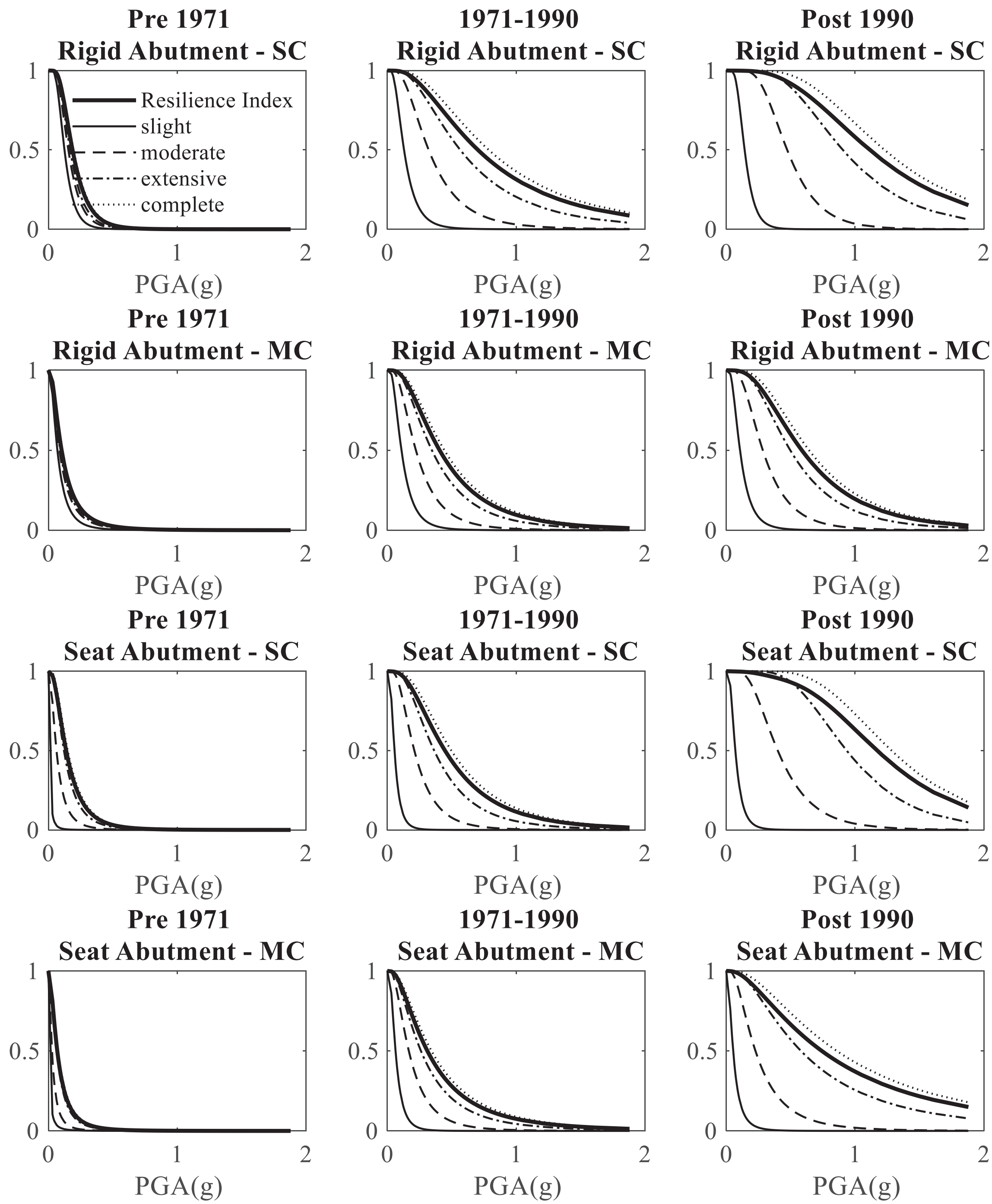

Fig. 9. Resilience Index vs probability of occurrence for each damage state.

$$MAPE = \frac{1}{n}\sum_{i=1}^{n}|y_i - \widehat{y}_i| \tag{9}$$

In this equation, y_i and $\widehat{y}_i$ represents the i^{th} data point and its predicted values, respectively, where n shows the total number of data points. These statistical indicators are provided in Tables 4 and 5 and Fig. 10.

Overall, the results indicate that the ensemble models captured good results in terms of accuracy, MSPE, and MAPE. Although among the explored algorithms, there is not a single model that is constantly superior to the others, bagging models, with the highest prediction accuracy (82%-95%) and lowest MSPEs and MAPEs (0.002–0.006 and 0.022–0.045), take the first place for almost all scenarios. However, since the three EL-based models demonstrated comparable performance for all bridge cases, we could conclude that bagging, boosting and random forest can provide efficient alternatives to the resilience quantification approach as explained in Section 2. For example, for the post-1990 bridge type with the rigid diaphragm abutment, the difference between the accuracy of predictions provided by bagging is slightly (1% and 3%, respectively) higher than those obtained from boosting and random forest. Overall, the accuracy varies within 1 to 7 percentage among the three EL-based models.

5.3. *Influential features*

An essential step to better interpret the results obtained by the ML

Table 3
The list of input variables for the resilience models.

Input variables	Seismic analysis characteristic	Input variables	Seismic analysis characteristic
x_1	Soil type	x_9	Reinforcement ratio
x_2	Girder type	x_{10}	Abutment height
x_3	Span length	x_{11}	Foundation translational stiffness
x_4	Column height	x_{12}	Foundation rotational stiffness
x_5	Deck width	x_{13}	Concrete strength
x_6	Superstructure depth	x_{14}	Reinforcement strength
x_7	Number of columns per bent	x_{15}	Abutment stiffness
x_8	Column diameter	x_{16}	PGA

Table 4
Evaluation of the predictive models (prediction accuracy comparison).

Bridge type	Bagging	Least-Squares Boosting	Random Forest
Pre 1971 – Rigid Diaphragm Abutment	0.820	0.784	0.789
1971–1990 – Rigid Diaphragm Abutment	0.915	0.892	0.862
Post 1990 – Rigid Diaphragm Abutment	0.948	0.937	0.918
Pre 1971 – Seat Abutment	0.826	0.802	0.754
1971–1990 – Seat Abutment	0.915	0.867	0.849
Post 1990 – Seat Abutment	0.935	0.909	0.895

Table 5
Evaluation of the predictive models (MSPE comparison).

Bridge type	Bagging	Least-Squares Boosting	Random Forest
Pre 1971 – Rigid Diaphragm Abutment	0.005	0.008	0.012
1971–1990 – Rigid Diaphragm Abutment	0.006	0.008	0.011
Post 1990 – Rigid Diaphragm Abutment	0.003	0.002	0.006
Pre 1971 – Seat Abutment	0.005	0.007	0.009
1971–1990 – Seat Abutment	0.002	0.004	0.011
Post 1990 – Seat Abutment	0.002	0.004	0.007

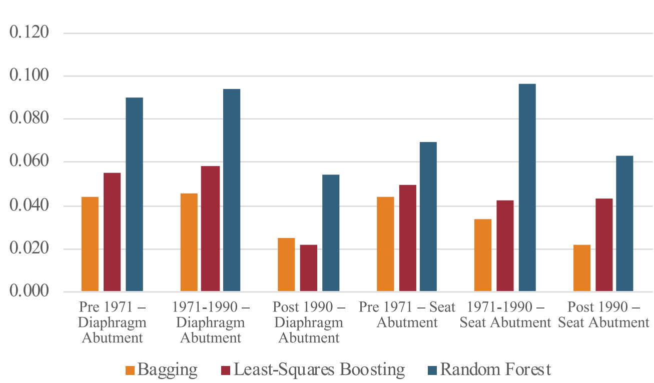

Fig. 10. Evaluation of the predictive models (MAPE comparison).

approaches is to assess the contribution of input bridge characteristics to predicting resilience index. In addition to better understanding the most influential parameters in determining bridge resilience, the input variables with a negligible relevant contribution can be identified so that they can be excluded to reduce model complexity and optimize model efficiency. To measure the level of importance of the variables, the EL algorithm, random forest, permutes the variables to monitor the averaged changes of the prediction errors and node impurities during the splitting process over all trees. Fig. 11 displays the importance of the variables measured using EL algorithms. These importance scores report the variance reduction due to the splits of a particular variable in the growth of regression trees. This implies how each variable decreases the impurity of the split. For each variable, the importance measure is averaged over all constructed trees. The values reported in Fig. 11 are the relative values (in percentages) of the computed importance measures that indicates the level of contribution of each variable in predicting the outcome. A larger variable importance score indicates a bigger contribution in the prediction.

In general, the most predictive parameters are the PGA and number of column bents, while the least predictive ones are the types of soil (sand or clay) and girder (prestressed or reinforced concrete). The influence of PGA can be explained by the importance of fragility curves in resilience index calculation, as shown and demonstrated in Fig. 7. While both PGA and structural parameters influence the shape of the fragility curves, in comparison to PGA, the impact of structural characteristics manifests in a gradual and subtle change in fragility curves. Hence, the influence of structural parameters on the resilience index is relatively smaller than PGA. Furthermore, the well-known recovery projection patterns utilized in this study are a function of damage state only. This can be further improved by defining and formulating the recovery projections as a function of different structural forms and characteristics; however, this is beyond the scope of this study. Further reflection in this figure shows that reinforcement ratio and superstructure depth are placed in the list of top five influential features for most cases. Foundation translational stiffness is also found in the high-rank parameters for bridges associated with the pre-1971 and 1971–1990 eras. Column height is found more significantly influencing the resilience of bridges with rigid diaphragm abutment than those with seat type abutments. In the case of bridges with seat abutments, column height is shown to have a greater influence on the resilience of bridges designed in earlier eras than the more recently constructed ones. On the contrary, deck width is found more influential for bridges with seat abutments than those with rigid diaphragms.

The observed differences could be related to a higher vulnerability of some components of bridges, particularly the columns when they have been designed in earlier eras compared to those that belong to a more recent, advanced seismically-designed period. The differences between the results of bridges with seat and rigid abutments could be related to their structural performance when subjected to excitation. Since the rigid abutment is integrally connected to the bridge superstructure they move synchronically in a seismic event, while the seat abutment and the superstructure move independently of each other.

6. Conclusion

This paper explored the potential application of ensemble learning (EL) based machine learning (ML) algorithms including bagged and boosted trees and random forest to provide a reliable prediction of the seismic resilience of bridges. Sixteen parameters were investigated, as the input variables for developing the EL-based models. These parameters are involved in the process of analytical development of probabilistic seismic demand and fragility curves of bridges which are used to quantify the seismic resilience of bridges.

To evaluate and verify the prediction capability of the EL-based models, the performance of the developed models was assessed via their prediction accuracies and the mean squared and relative errors. According to the comparisons, the three proposed EL-based predictive resilience models successfully predicted bridge seismic resilience, with an average accuracy greater than 84%, and generally performed well considering all three statistical indicators. Although the prediction accuracy does not vary significantly from one method to another, the results show that the bagged trees-based model offers a lower means

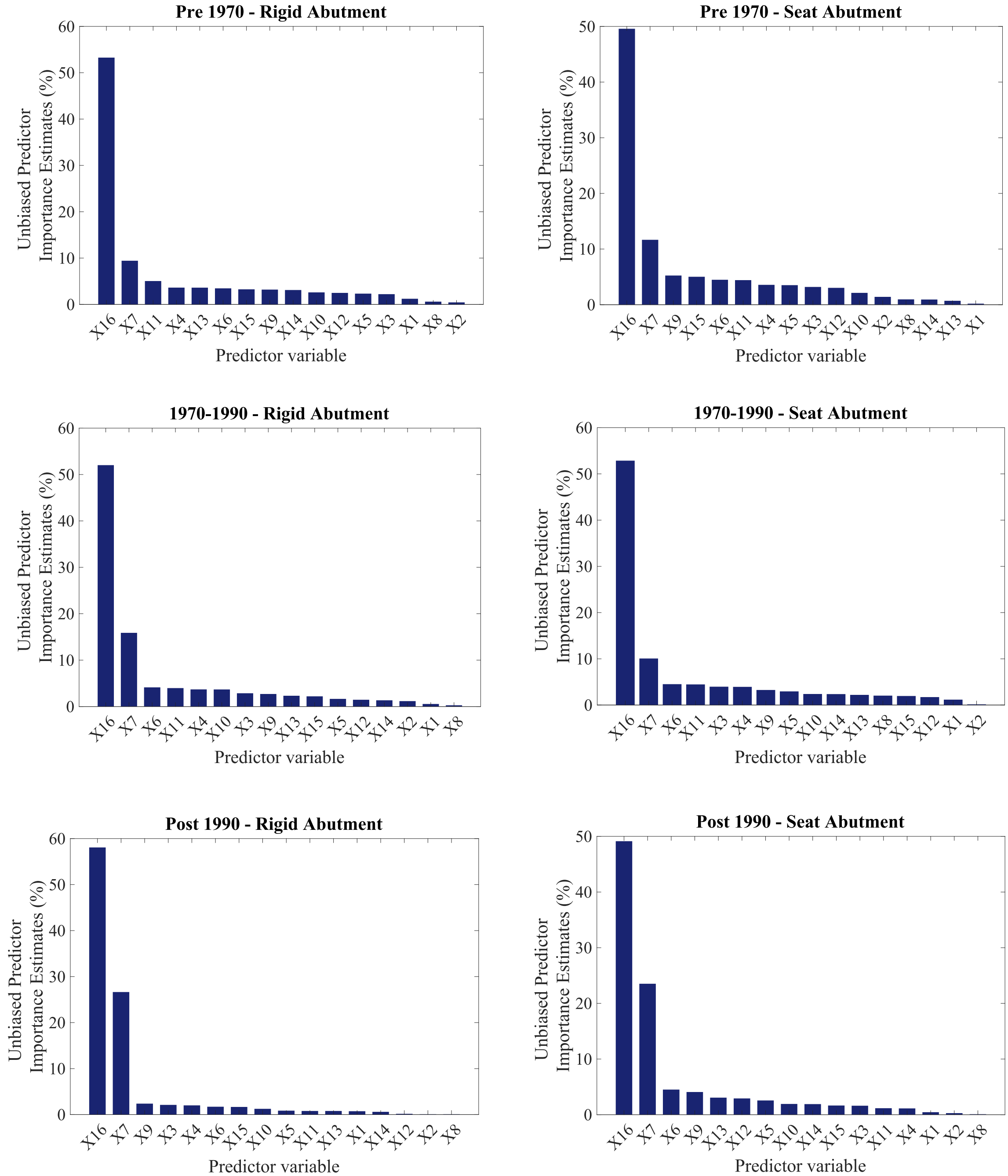

Fig. 11. Features ranking based on their level of importance measures in predicting bridge resilience.

squared and relative errors in comparison to other models, hence providing a consistently superior prediction performance in all bridge types. This suggests that the nature of the resilience metric used in this study is better predicted by a multi decision tree classifier as it reduces the likelihood of over-fitting. This method also performs better for high-dimensional input data.

Moreover, the feature importance of the considered variables was measured, and a ranking based on the level of contribution that each variable has in predicting the seismic resilience of bridges was provided. The intuition from the features ranking and the identification of the most and least influential parameters is beneficial to making informed decisions in the resilience assessment of bridges and developing parsimonious models. The ground motion intensity (PGA) and the number of bridge columns per bent were identified as the most influential features by taking first place in all investigated scenarios. Furthermore, the type of superstructure girder and soil had the lowest contribution in the predictions.

This study presented EL-based methodologies to provide insights towards the application of ML algorithms in the seismic resilience assessments of bridges. Future studies on the vulnerability assessment of the bridge system can address the limitations of the presented work. For example, while this study confirmed the efficiency of EL-based methods in predicting the seismic resilience of box-girder bridges, the generalization of the findings from this study can be tested by analyzing other bridge types such as I- and T-girder bridges. Besides, future works can investigate the sensitivity of bridge resilience to different ground motion characteristics, in addition to the considered PGA in this study.

Declaration of Competing Interest

The authors declare that they have no known competing financial interests or personal relationships that could have appeared to influence the work reported in this paper.

Appendix A

This appendix presents the general modeling properties of the considered concrete box-girder bridges. More details about the bridge modeling procedure and the bridge characteristics can be found in previous works (Ramanathan, 2012; Soleimani, 2017). A uniform distribution is considered for the longitudinal reinforcement ratio of the columns with the lower and upper bounds equal to 1.4 and 2.4, 1.0 and 3.7, and 1.0 and 3.5 for pre 1971, 1971-1990, and post 1990 design eras, respectively. For the transverse reinforcement ratios, #4 stirrups with 12-inch spacing are adopted for bridges designed before 1971. However, uniform distribution with lower and upper bounds of 0.3 and 0.9, and 0.4 and 1.7 are considered for the 1971-1990 and post 1990 eras.

Table A.1
General bridge modeling properties (Ramanathan, 2012; Soleimani, 2017).

Bridge parameters	Distribution	Units	Mean	Standard deviation
Concrete compressive strength	Normal	ksi	5.0	0.63
Reinforcing steel yield strength	Lognormal	ksi	4.21	0.08
Span length	Empirical	ft	114.8	40.5
Deck width	Empirical	ft	67.2	42.2
Vertical under clearance	Empirical	ft	18.0	3.7
Abutment concrete pile effective stiffness	Lognormal	kip/in	80.0	0.3
Damping	Normal	-	0.045	0.0125

Table A.2
General bridge modeling properties (Ramanathan, 2012; Soleimani, 2017).

Bridge parameters	Distribution	Units	Lower bound	Upper bound
Shear modulus of elastomeric bearing pads	Uniform	ksi	80	250
Abutment backwall height	Uniform	ft	3.5	8.5
Gap between deck and seat type abutment backwall	Uniform	in	0	1.5
Restrainer cable length	Uniform	ft	8	20
Mass factor	Uniform	-	1.1	1.4

Table A.3
Component capacities adopted in this study (Ramanathan, 2012; Soleimani, 2017).

Engineering demand parameter	Eras	Units	DS1	DS2	DS3	DS4
Column curvature ductility	Pre 1971	NA	0.8	0.9	1.0	1.2
	1971-1990	NA	1.0	2.0	3.5	5.0
	Post 1990	NA	1.0	4.0	8.0	12.0
Deck displacement	All	Inches	1.0	3.0	10.0	15.0
Foundation rotation	All	Radian	1.5	6.0	NA	NA
Foundation displacement	All	Inches	1.0	4.0	NA	NA
Bearing displacement	All	Inches	1.0	4.0	NA	NA
Abutment passive displacement	All	Inches	3.0	10.0	NA	NA
Abutment active displacement	All	Inches	1.5	4.0	NA	NA
Abutment transverse displacement	All	Inches	1.0	4.0	NA	NA

References

[1] Altman N, Krzywinski M. Ensemble methods: bagging and random forests. Nat Methods 2017;14(10):933–4.
[2] Biondini F, Camnasio E, Titi A. Seismic resilience of concrete structures under corrosion. Earthquake Eng Struct Dyn 2015;44(14):2445–66.
[3] Bocchini P, Frangopol DM. Optimal resilience-and cost-based postdisaster intervention prioritization for bridges along a highway segment. J Bridge Eng 2012;17(1):117–29.
[4] Bocchini P, Decò A, Frangopol DM. Probabilistic functionality recovery model for resilience analysis. Bridge maintenance, safety, management, resilience and sustainability 2012:1920–7.
[5] Butler D, Farmani R, Fu G, Ward S, Diao K, Astaraie-Imani M. A newapproach to urban water management: safe and sure. Procedia Eng. 2014;89:347–54.
[6] Breiman L, Friedman J, Stone CJ, Olshen RA. Classification and regression trees. CRC Press; 1984.
[7] Breiman L. Bagging predictors. Machine Learning 1996;24(2):123–40.
[8] Bühlmann P. Bagging, boosting and ensemble methods. In: Gentle JE, Härdle WK, Mori Y, editors. Handbook of Computational Statistics. Berlin, Heidelberg: Springer Berlin Heidelberg; 2012. p. 985–1022. https://doi.org/10.1007/978-3-642-21551-3_33.
[9] Chandrasekaran S, Banerjee S. Retrofit optimization for resilience enhancement of bridges under multihazard scenario. J Struct Eng 2016;142(8):C4015012.
[10] Chiou B, Darragh R, Gregor N, Silva W. NGA project strong-motion database. Earthquake Spectra 2008;24(1):23–44.
[11] Department for Transport. (2014). Transport Resilience Review: A review of the resilience of the transport network to extreme weather events. Available online: https://assets.publishing.service.gov.uk/government/uploads/system/uploads/attachment_data/file/335115/transport-resilience-review-web.pdf.
[12] Decò A, Bocchini P, Frangopol DM. A probabilistic approach for the prediction of seismic resilience of bridges. Earthquake Eng Struct Dyn 2013;42(10):1469–87.
[13] Dietterich TG (2000). Ensemble methods in machine learning. In International workshop on multiple classifier systems (pp. 1-15). Springer, Berlin, Heidelberg.
[14] Dong Y, Frangopol DM. Risk and resilience assessment of bridges under mainshock and aftershocks incorporating uncertainties. Eng Struct 2015;83:198–208.
[15] Fawagreh K, Gaber MM, Elyan E. Random forests: from early developments to recent advancements. Systems Sci Control Eng: An Open Access Journal 2014;2(1):602–9.
[16] FEMA. (2009). HAZUS-MH MR4–Earthquake Model User Manual.
[17] Freddi F, Padgett JE, Dall'Asta A. (2017). Probabilistic seismic demand modeling of local level response parameters of an RC frame. Bull Earthquake Eng, 15(1), 1-23.
[18] Gardoni P, Mosalam KM, Der Kiureghian A. Probabilistic seismic demand models and fragility estimates for RC bridges. J Earthquake Eng 2003;7(sup001):79–106.
[19] Gidaris I, Padgett JE, Barbosa AR, Chen S, Cox D, Webb B, et al. Multiple-hazard fragility and restoration models of highway bridges for regional risk and resilience assessment in the United States: state-of-the-art review. J Struct Eng 2017;143(3):04016188. https://doi.org/10.1061/(ASCE)ST.1943-541X.0001672.
[20] Hajializadeh D, Imani M. RV-DSS: Towards a resilience and vulnerability-informed decision support system framework for interdependent infrastructure systems. Comput Ind Eng 2020;156:107276.
[21] Hancock T, Put R, Coomans D, Vander Heyden Y, Everingham Y. A performance comparison of modern statistical techniques for molecular descriptor selection and retention prediction in chromatographic QSRR studies. Chemometrics and Intelligent Laboratory Systems 2005;76(2):185–96.
[22] Harrou F, Saidi A, Sun Y. Wind power prediction using bootstrap aggregating trees approach to enabling sustainable wind power integration in a smart grid. Energy Convers Manage 2019;201:112077. https://doi.org/10.1016/j.enconman.2019.112077.
[23] Hastie T, Tibshirani R, Friedman J. Random forests. In: The elements of statistical learning. New York, NY: Springer; 2009. p. 587–604.
[24] HAZUS-MH. (2011). Multi-hazard loss estimation methodology: Earthquake model Hazus-MH MR5 technical manual.
[25] Henry D, Emmanuel Ramirez-Marquez J. Generic metrics and quantitative approaches for system resilience as a function of time. Reliab Eng Syst Saf 2012;99:114–22.
[26] Hosseini S, Barker K, Ramirez-Marquez JE. A review of definitions and measures of system resilience. Reliab Eng Syst Saf 2016;145:47–61.
[27] Housner GW, Thiel CC. The continuing challenge: Report on the performance of state bridges in the Northridge earthquake. Earthquake Spectra 1995;11(4):607–36.
[28] Kafali C, Grigoriu M. Rehabilitation decision analysis. ICOSSAR'05: Proceedings of the Ninth International Conference on Structural Safety and Reliability. 2005.
[29] Karamlou A, Bocchini P. Computation of bridge seismic fragility by large-scale simulation for probabilistic resilience analysis. Earthquake Eng Struct Dyn 2015;44(12):1959–78.
[30] Kawashima K, Unjoh S, Hoshikuma J-I, Kosa K. Dam- age of bridges due to the 2010 Maule, Chile, earthquake. J Earthquake Eng 2011;15(7):1036–68.
[31] Lerman RI, Yitzhaki S. A note on the calculation and interpretation of the Gini index. Econ Lett 1984;15(3-4):363–8.
[32] Li Z, Goebel K, Wu D. Degradation modeling and remaining useful life prediction of aircraft engines using ensemble learning. J Eng Gas Turbines Power 2019;141(4).
[33] Liu Y, Wang Y, Zhang J. In: September). New machine learning algorithm: Random forest. Berlin, Heidelberg: Springer; 2012. p. 246–52.
[34] Meir R, Rätsch G. An introduction to boosting and leveraging. In: Advanced lectures on machine learning. Berlin, Heidelberg: Springer; 2003. p. 118–83.

[35] Mackie K, Stojadinović B. Probabilistic seismic demand model for California highway bridges. J Bridge Eng 2001;6(6):468–81.
[36] Mahjoobi J, Etemad-Shahidi A, Kazeminezhad MH. Hindcasting of wave parameters using different soft computing methods. Appl Ocean Res 2008;30(1): 28–36.
[37] Mangalathu S, Soleimani F, Jeon JS. Bridge classes for regional seismic risk assessment: Improving HAZUS models. Eng Struct 2017;148:755–66.
[38] NBI. National bridge inventory data. US Dept. of Transportation, Federal Highway Administration, Washington, DC; 2010. <http://www.fhwa.dot.gov/ bridge/nbi/ ascii.cfm>.
[39] Nielson BG, DesRoches R. Seismic fragility methodology for highway bridges using a component level approach. Earthquake Eng Struct Dyn 2007;36(6):823–39.
[40] Padgett JE, DesRoches R. Sensitivity of seismic response and fragility to parameter uncertainty. J Struct Eng 2007;133(12):1710–8.
[41] Padgett JE, Nielson BG, DesRoches R. Selection of optimal intensity measures in probabilistic seismic demand models of highway bridge portfolios. Earthquake Eng Struct Dyn 2008;37(5):711–25.
[42] Ramanathan KN. Next generation seismic fragility curves for California bridges incorporating the evolution in seismic design philosophy (Doctoral dissertation). Georgia Institute of Technology; 2012.
[43] Schanack Frank, Valdebenito Galo, Alvial Jorge. Seismic damage to bridges during the 27 February 2010 magnitude 8.8 Chile earthquake. Earthquake Spectra 2012; 28(1):301–15.
[44] Schapire RE. The boosting approach to machine learning: An overview. Nonlinear estimation and classification 2003:149–71.
[45] SDC. Seismic design criteria. Version 1.6. California Department of Transportation, Sacramento, CA; 2010.
[46] Sharma N, Tabandeh A, Gardoni P. Resilience analysis: A mathematical formulation to model resilience of engineering systems. Sustainable and Resilient Infrastructure 2018;3(2):49–67.
[47] Shome N, Cornell CA, Bazzurro P, Carballo JE. Earthquakes, records, and nonlinear responses. Earthquake Spectra 1998;14(3):469–500.
[48] Skurichina M, Duin RP. (2002). Bagging, boosting and the random subspace method for linear classifiers. Pattern Analysis & Applications, 5(2), 121-135.
[49] Soleimani F. Fragility of California bridges-development of modification factors (Doctoral dissertation). Georgia Institute of Technology; 2017.
[50] Soleimani F. Propagation and quantification of uncertainty in the vulnerability estimation of tall concrete bridges. Eng Struct 2020;202:109812. https://doi.org/10.1016/j.engstruct.2019.109812.
[51] Soleimani, F. (2021, August). Analytical seismic performance and sensitivity evaluation of bridges based on random decision forest framework. In Structures (Vol. 32, pp. 329-341). Elsevier.
[52] Soleimani F, Liu X. Artificial neural network application in predicting probabilistic seismic demands of bridge components. Earthquake Eng Struct Dyn 2021.
[53] Soleimani F, Macedo J, Liu C. Machine learning-based selection of efficient parameters for the evaluation of seismically-induced slope displacements. ASCE Lifelines Conference. 2022.
[54] Soleimani F, Mangalathu S, DesRoches R. A comparative analytical study on the fragility assessment of box-girder bridges with various column shapes. Eng Struct 2017;153:460–78.
[55] Soleimani F, Vidakovic B, DesRoches R, Padgett JE. Identification of the significant uncertain parameters in the seismic response of irregular bridges. Eng Struct 2017; 141:356–72.
[56] Sun Q, Pfahringer B. Bagging ensemble selection for regression. In: Australasian Joint Conference on Artificial Intelligence. Berlin, Heidelberg: Springer; 2012. p. 695–706.
[57] Sutton CD. Classification and regression trees, bagging, and boosting. Handbook of statistics 2005;24:303–29.
[58] Syam N, Kaul R. (2021). Random Forest, Bagging, and Boosting of Decision Trees. In Machine Learning and Artificial Intelligence in Marketing and Sales. Emerald Publishing Limited.
[59] Venkittaraman A, Banerjee Sw. Enhancing resilience of highway bridges through seismic retrofit. Earthquake Eng Struct Dyn 2014;43(8):1173–91.
[60] Woods DD. Four concepts for resilience and the implications for the future of resilience engineering. Reliab Eng Syst Saf 2015;141:5–9.
[61] Yang P, Hwa Yang Y, Zhou B, Y Zomaya A. (2010). A review of ensemble methods in bioinformatics. Curr Bioinformatics, 5(4), 296-308.
[62] Zhong J, Gardoni P, Rosowsky D, Haukaas T. Probabilistic seismic demand models and fragility estimates for reinforced concrete bridges with two-column bents. J Eng Mech 2008;134(6):495–504.
[63] Zhou Y, Banerjee S, Shinozuka M. Socio-economic effect of seismic retrofit of bridges for highway transportation networks: a pilot study. Struct Infrastruct Eng 2010;6(1-2):145–57.
[64] Zhou ZH. (2021). Ensemble learning. In Machine Learning (pp. 181-210). Springer, Singapore.
[65] Soleimani F. Probabilistic seismic analysis of bridges through machine learning approaches. Structures. Vol. 38. Elsevier; 2022. p. 157–67.
[66] Ishwaran H, Kogalur UB. Consistency of random survival forests. Statistics & probability letters 2010;80(13–14):1056–64.